基于可编程控制的扫描电子束加工技术

李少青， 王学东， 张毓新， 姚 舜
（上海交通大学 焊接工程研究所，上海 200030）

摘 要：在通用真空电子束焊机的基础上配置两对电子束偏转线圈、工控机多功能数据采集卡、功率放大器、可编程控制器以及虚拟仪器软件 LabVIEW 等，构建一个电子束扫描控制系统。利用该系统可对电子束扫描轨迹、扫描频率以及加热区域电子束能量密度的分配进行离线编辑和在线调节。使用该系统进行了不锈钢毛细管板结构的钎焊试验，钎焊接头质量满足结构技术规范。对铌钛异种合金采用不对称热输入的扫描加热方式进行焊接，获得了铌、钛熔化量相当，焊缝形状对称的焊接接头。对于不能直接焊接的异种金属（如 Re-Ti），可使用该系统的扫描加热技术，通过粉末冶炼制备中间过渡层。

关键词：电子束；扫描控制系统；扫描轨迹；能量控制
中图分类号：TG456.9 文献标识码：A 文章编号：0253-360X(2005)07-59-05

李少青

0 序 言

真空电子束焊因为能量密度高，热影响区窄，焊接变形小，广泛应用于不锈钢、合金钢、高熔点合金、有色金属材料的熔焊。对于需要不对称热输入异种金属焊接和需要局部区域均匀加热，或者按特殊路径扫描加热的真空电子束钎焊，通用真空电子束焊机由于受其扫描控制系统的限制，则难以胜任。尽管通用真空电子束焊机具有简单的扫描控制功能，可以生成正弦波、方波、圆等几种固定的扫描波形，但扫描范围有限。许多研究者为此进行长期不懈的研究，对电子束偏转控制系统进行一次一次革新[1~4]。电子技术、自动控制技术、计算机技术的高速发展，为电子束扫描加热过程的精确控制提供可行性。文中建立了一套基于虚拟仪器控制的柔性电子束扫描控制系统。利用该系统可对电子束扫描轨迹、扫描频率等进行离线编辑和在线调节，并可将电子束扫描三维能量密度分布显示在窗口中。该系统能适应焊缝形状复杂、接头输入能量配比可控以及大面积扫描加热的特殊加工要求，为电子束加工技术在钎焊、重熔、表面改性、异种金属焊接、快速成型等领域的应用创造了条件。

1 电子束扫描控制系统的组成

电子束扫描控制系统由电子束焊机、工业控制计算机（IPC）、NI（National Instruments 美国国家仪器公司）多功能数据采集卡、功率放大器、电子束偏转线圈、可编程序控制器等组成，如图 1所示。首先根据工件的加热要求，利用 LabVIEW 编辑出电子束扫描加热波形。程序运行过程中，IPC 计算波形数据并由数据采集卡转换为模拟信号，再经功率放大器放大后输送给电子束偏转线圈。X、Y 两对绕组置于电子枪外电子束运行路径上，分别控制电子束在 X、Y 方向的偏转，产生所需要的扫描轨迹。

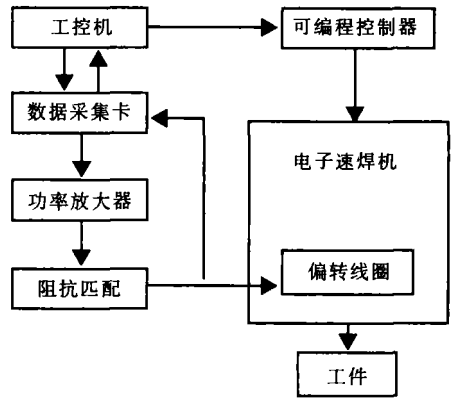

图 1 电子束扫描控制系统组成
Fig. 1 Diagram of EB scanning control system

2 电子束扫描控制系统的功能

2.1 扫描轨迹的表征

电子束扫描轨迹采用二维曲线来描述。在直角

收稿日期：2004-08-13

坐标系中建立电子束扫描轨迹的参数方程，然后对其坐标分量函数式进行离散化处理，将连续扫描轨迹用一系列点来描述，即

$$\begin{cases} X_i=\varphi(t_i) \\ Y_i=\psi(t_i) \end{cases},$$

式中：$i=0, 1, 2, \cdots, n-1$（n为扫描轨迹中包含点数）。由工控机计算出各点数据值后，用二维数组存储，然后再进行数模转换。

如果扫描轨迹是由几段曲线组成，且这几段具有不同的曲线方程形式，那么分别对各段的曲线方程进行离散化处理，然后再进行数据装配最终仍用一个二维数组来存储。

对于难以用数学函数表达的不规则扫描轨迹，则可以采用数据文件的形式来描述扫描轨迹，亦即数据文件本身就是离散化后的数字量，程序运行过程中直接由工控机读取其中的数值，不需再进行离散化处理。

2.2 扫描波形的实时调节和显示

通常，在真空电子束焊接过程中，通过操纵真空室中三维精密调节机构移动工件或电子枪的位置实现电子束焊缝位置的对中，但对一些形状比较复杂的扫描轨迹与焊缝的对中通过调节机构则很难满足控制精度要求。利用电子束扫描控制系统则可以通过扫描轨迹参数的实时调节来实现焊缝对中。

扫描轨迹的实时调节是指扫描轨迹参数配置、波形计算与实际扫描过程控制的在线调节，当预置扫描轨迹参数给定或轨迹参数修改后，扫描轨迹可以立即生成，通过轨迹相对于焊缝移动、旋转，从而使扫描轨迹与实际焊缝位置精确吻合，即使在随后的焊接过程中也能根据需要调节轨迹及波形各参数，如扫描频率、点数等。

扫描波形显示是除扫描轨迹实时调节之外另一种必要的控制手段。工控机所发出的两路模拟信号在传送给偏转线圈之前，先通过数据采集卡的模拟量输入通道采集 X、Y 两路模拟驱动信号，转换合成并显示在工控机屏幕上，在对工件施加预置束流焊接之前可以采用小束流对扫描轨迹初步配置进行评估，减少试验时间，提高效率。

2.3 能量控制

电子束的能量密度分布是决定焊接温度场的主要因素之一，能量分布取决于电子束束流大小，扫描轨迹形状、尺寸，扫描频率及加热时间等因素。电子束扫描控制系统以扫描轨迹中的各点为研究对象，计算出各点的能量分布，从而求出整个扫描轨迹中的能量分布。

利用该系统可进行扫描轨迹的能量分布预测，并在工控机屏幕上实时显示出来。当扫描加热参数变化时，能量分布自动重新计算。根据具体要求，将能量分布以三维空间或二维平面坐标形式显示在窗口中。

3 系统在材料加工中的应用

3.1 毛细管板接头电子束钎焊

利用电子束扫描控制系统进行了毛细管板结构的真空电子束钎焊试验。板材和毛细管材质均为1Cr18Ni9Ti，试板规格为 ϕ40mm×5mm，试板中间部位开三个毛细管安装小孔。毛细管外径 0.5mm，壁厚 0.1mm，与试板间的装配间隙为 0.03mm。钎料选用粉末状 BNi-2。将 25mg钎料用粘结剂调成膏状，涂敷在试板背面毛细管周围。针对毛细管板结构特点，为了三管同时均匀加热，编辑成三瓣形的扫描轨迹，如图 2a所示。焊接过程中，通过扫描轨迹移动、旋转以及尺寸的实时调节，使三根毛细管分别位于三个圆形叶瓣的中心，然后采用设定的焊接参数，在工件正面进行扫描加热。当毛细管周围区域加热到钎焊温度，涂敷在工件背面毛细管周围的钎料熔化，液态钎料在毛细作用下流入并填满装配间隙，爬升到工件正面，完成真空电子束钎焊过程。钎焊过程中电子束实际扫描加热轨迹如图 2b所示。

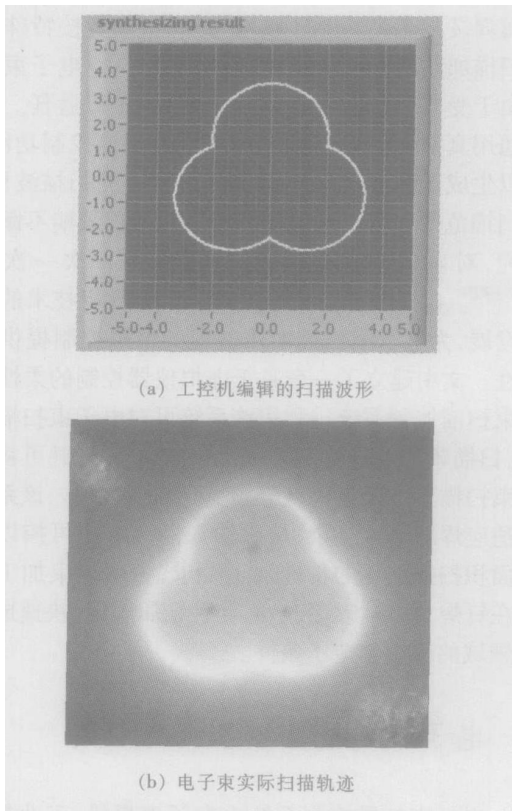

图 2 电子束钎焊扫描轨迹

Fig. 2 Scanning track of electron beam brazing

对于试验毛细管板结构，通过一系列工艺试验，得出真空电子束钎焊优化工艺参数为：加速电压 60 kV，束流 6.5mA，加热时间 40 s，聚焦电流 564 mA，电子束扫描幅值 0.5。毛细管板接头的钎焊试验结果表明，接头部位的钎缝均匀圆滑，钎透率 100%。在此电子束钎焊规范下，工件在钎料熔点（980 ℃）以上温度停留的时间为 20 s左右，而 BNi-2钎料真空钎焊不锈钢的钎焊规范一般为 1 050 ℃（或 1120 ℃），保温 10 min[5]。因此，与传统真空炉钎焊相比，电子束钎焊升温速度快，高温停留时间要短得多，不易造成薄壁毛细管溶蚀。

3.2 铌合金与钛合金的电子束焊接

铌合金与钛合金具有相同的 Ti、Nb、Zr等元素，冶金性能比较接近，不会产生脆性金属间相，可形成有限固溶体，理论上可焊性较好。但是两种合金熔点相差较大，热传导性能也有差别，焊接时应减少钛合金一侧的能量输入，从而可平衡这两种合金热物理性能差别的影响，防止两种合金熔合不充分[6]。

铌-钛焊接接头结构如图 3所示。采用传统电子束焊接方法沿焊缝进行焊接，铌合金与钛合金两侧能量输入相等，难以保证接头的焊接质量，焊接结果如图 4a所示。而采用电子束扫描控制系统则可以改变电子束焊接典型高斯分布温度场形态，对熔点高的一侧能量输入大一些，熔点低一侧能量输入小一些，实现接头焊缝的良好对称性。图 5为铌-钛电子束焊接扫描波形。焊接过程中，电子束沿焊缝两侧对铌合金与钛合金进行高速扫描加热，通过调整方波的上、下幅值（即电子束在焊缝两侧的偏移距离）和占空比（即电子束在焊缝两侧停留时间之比）来控制铌-钛两侧的能量输入分布的形态。采用与图 4a相同的焊接参数，通过不对称的能量输入控制，获得了铌钛熔化量相当、焊缝形状比较对称的焊接接头，如图 4b所示。

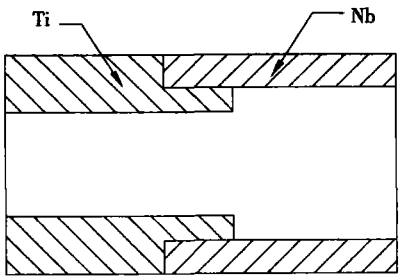

图 3　铌合金与钛合金接头示意图

Fig.3　Diagram of Nb-Ti joint

3.3 粉末熔炼制备过渡层

对于不能直接焊接的异种金属，如铼和钛合金，必须设计和制备合适的过渡层材料。铼和钛物理性能如表 1所示，物理性能和结晶化学性的差异，使其在冶金学上的相容性差，在铼中会形成脆性 ω 相，在铼钛接头中会产生 Ti_5Re_{24}金属间化合物，导致接头产生裂纹，强度大大下降。因此须按一定配比制备中间过渡层材料，抑制熔焊接头中脆性相形成。由于 Re、Ti合金的熔点非常高，采用 2000 ℃以上的烧结温度的粉末冶金方法制备中间过渡层难以实现。利用电子束扫描控制系统，通过可控电子束扫描加热熔炼金属粉末，解决高熔点的复合过渡层制备问题。

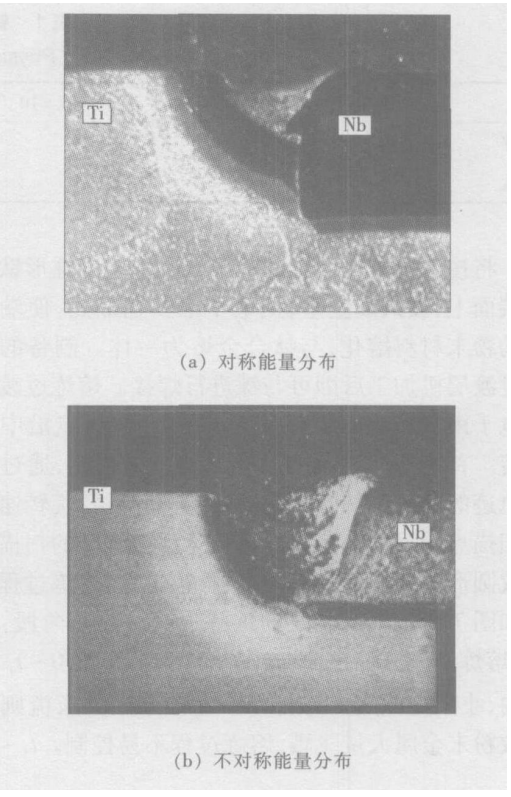

图 4　铌合金与钛合金电子束焊接接头

Fig.4　Nb-Ti EBW joint

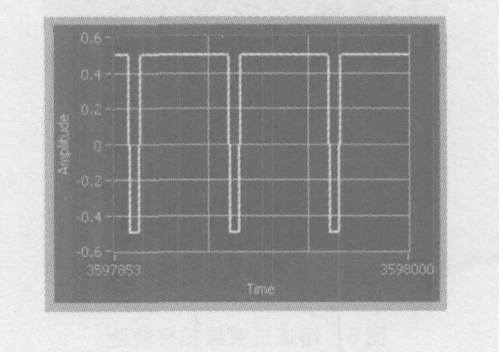

图 5　铌合金与钛合金电子束焊接扫描波形

Fig.5　Scanning waveform for Nb-Ti EBW

表 1 铼、钛主要物理性能

Table 1 Physical properties of Re and Ti

	熔点 T_M /℃	线膨胀系数 α /(℃$^{-1}$×10^{-6})	比热 C /(J·kg^{-1}·℃$^{-1}$)	热导率 λ /(W·m^{-1}·℃$^{-1}$)
铼	3 186	6.6~6.8	137	71.1
钛	1 670	8.41	544.28	15.06

将按一定配比混合的粉末金属置于圆柱形钛合金端面上,放入真空室,用电子束扫描加热,使端面上的粉末材料熔化,与钛合金熔为一体。制备的复合过渡层机加工后即可与铼进行焊接。熔炼过渡层的电子束扫描轨迹如图 6所示,四个扫描点沿中心旋转。首先根据工件的尺寸以及材料性能,通过扫描轨迹的实时调节,确定扫描轨迹的半径、旋转速度和扫描点的尺寸等参数。熔炼过程中旋转的扫描点形成圆形的扫描面,将过渡层材料熔化,熔炼过程照片如图 7所示。过渡层的熔炼过程分三个阶段:预热、熔炼和成分稳定化,如图 8所示。首先,0~t_1时间内,小束流预热,否则,如果直接采用大束流则会导致粉末金属大量飞溅,熔炼过程不易控制。t_1~t_2时间内,大束流加热熔炼,直至过渡层全部熔化。t_2~t_3时间为成分稳定化阶段,适当减小束流。采用电子束扫描控制系统,可以通过电子束束流大小,扫描轨迹形状、尺寸,扫描频率及加热时间等因素的调节,控制电子束输入能量的分布,从而控制基体材料对中间层的稀释率,最终达到控制中间层成分的目的。试验结果表明,用受控电子束熔炼粉末金属可以获得满意的中间过渡层,如图 9所示。

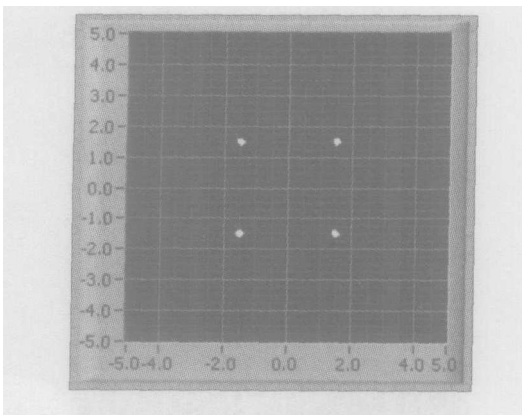

图 6 熔炼过渡层扫描轨迹

Fig. 6 Scanning track for smelting transition layer

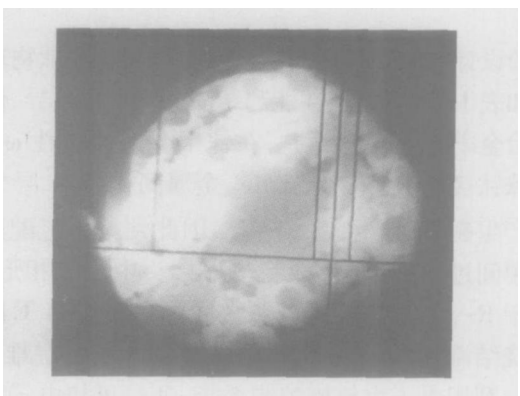

图 7 熔炼过程照片

Fig. 7 Photograph of smelting process

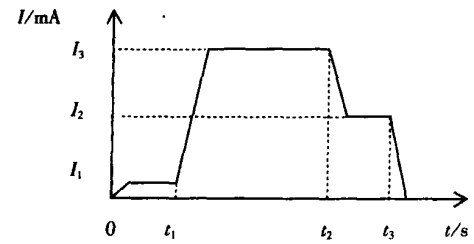

图 8 过渡层熔炼过程

Fig. 8 Smelting process of transition layer

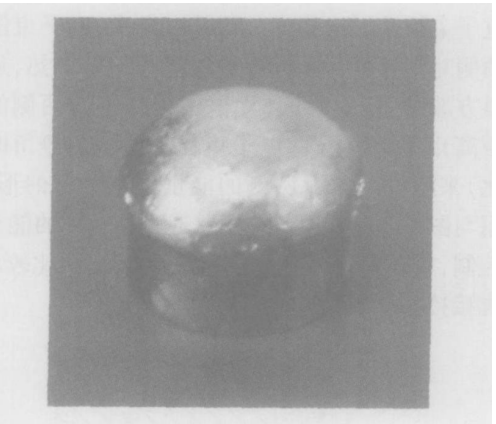

图 9 钛合金及过渡层

Fig. 9 Ti alloy with transition layer

4 结 论

(1) 所建立的电子束扫描控制系统可以编辑生成所需形状的扫描轨迹,通过 LabVIEW 虚拟仪器控制可实时调整扫描轨迹波形,显示在窗口中,通过能量密度计算,且可将电子束扫描三维能量分布显示

[下转第 66页]

HV,然后又逐渐下降到 380 HV左右。这个峰值的出现可能是因为在此处生成的(NiTi+ Ni3Ti)相中弥散分布着母材 TC4扩散过来 Al和夹层扩散过来的 Ni等元素,起到弥散强化的作用。

3 结 论

(1)在连接温度 870 ℃,连接压力 10MPa,保温时间 60min的工艺参数下,采用 Ni箔做中间层在真空下能够实现 TC4和 QAl10-3-1.5扩散连接,抗拉强度达到了 325MPa。

(2) TC4/Ni/QAl10-3-1.5扩散连接接头形成明显的过渡扩散区域,从 TC4到 QAl10-3-1.5反应层的相结构有:NiTi相,(NiTi+Ni3Ti)相,拉伸试验表明断口发生在 TC4/Ni生成的金属间化合物处。同时在 Ni/QAl10-3-1.5扩散层形成了 Ni(Cu)固溶体。

(3)元素扩散对 TC4/QAl10-3-1.5扩散连接接头的硬度影响很大,在 Ni夹层的两端都形成了一个峰值,在 Ni/QAl10-3-1.5之间由于 Ni,Cu两种元素的固溶强化硬度提高, TC4/Ni之间弥散分布着 Ni,Al等元素弥散强化的作用所致。

参考文献:

[1] Peng He, Jiuhai Zhang, Ronglin Zhou, *et al*. Diffusion bonding technology of a titanium alloy to a stainless steel web with an Ni interlayer[J]. Materials Characterization, 1999, (43): 287-292.

[2] He P, Feng J C, Zhang B G, *et al*. Microstructure and strength of diffusion-bonded joints of TiAl base alloy to steel[J]. Materials Characterization, 2002, (48): 401-406.

[3] Uzunov Tz D, Lambov S I, Stojanov S T P. Kinetics of solid-phase interactions in thin-film Cu/Ti system with a excess of Ti[J]. Vacuum, 1995, 46(11): 1347-1350.

[4] Uzunov Tz D, Lambov S I, Stojanov S T P. Kinetics of solid phase interactions in thin-film Cu/Ti system with a excess of Cu[J]. Vacuum, 1996, 47(1): 61-65.

[5] Sun Ronglu, Li Muqin, Zhang Jiuhai, *et al*. Influence of different transition metals on properties of diffusion bonding joint of Ti alloy to stainless steel[J]. Transactions of the China Welding Institution, 1996, 12(4): 25-28.
孙荣禄,李幕勤,张九海,等. 中间过渡金属对钛合金与不锈钢扩散焊接头强度的影响[J]. 焊接学报, 1996, 12(4): 25-28.

作者简介:郭 伟,男,1976年出生,在读博士研究生,主要研究方向为新型材料的扩散连接、钎焊工艺。

Email: gwlunar@sohu.com

[上接第 62页]

在窗口中。

(2)采用电子束扫描控制系统,成功实现毛细管板结构的真空电子束钎焊,不但有效避免了毛细管的溶蚀、烧穿和堵塞等缺陷,而且可以大大提高钎焊工作效率。

(3)采用电子束扫描控制系统可对电子束能量输入分布进行控制,解决物理性能差异较大的异种金属的焊接问题,实现接头焊缝的良好对称性。

(4)利用电子束扫描控制系统的扫描轨迹旋转功能可进行高熔点粉末金属熔炼。对于不能直接焊接的异种金属,通过粉末金属熔炼制备满意的中间过渡层。

参考文献:

[1] Bahr M, Hoffmann G, Ludwig R, *et al*. New scan and control system for high power electron beam techniques[J]. Surface and Coating Technology, 1998, 22(8): 1211-1220.

[2] Steffen Keitel, Gotz Sobisch, Andreas Hankle, *et al*. Shaping of deflection figures of electron beam equipment[J]. Schweissen-Schneiden with English Translation, 1998, 50(8): 150-153.

[3] Jan Dupák, Ivan Vlcek, Martin Zobac. Electron gun for computer-controlled welding of small components[J]. Vacuum, 2001, 62(6): 159-164.

[4] Guo Guangyao, Liu Fangjun, Han Ruiqing. Control system for electron beam scan[J]. Transactions of the China Welding Institution, 2003, 24(1): 91-93.
郭光耀,刘方军,韩瑞清. 电子束扫描控制系统[J]. 焊接学报, 2003, 24(1): 91-93.

[5] 庄鸿寿, E. 罗格夏特. 高温钎焊[M]. 北京:国防工业出版社, 1989. 25-85.

[6] 胡振海,朱铭德,张建浩. 钛合金与铌合金的真空电子束焊接工艺[J]. 航天工艺, 2001, 1: 10-15.

作者简介:李少青,女, 1979年 1月出生,博士研究生。研究方向为高能束焊接及复合工艺、焊接过程数值分析。已发表论文 10余篇。

Email: lishaoqing@sjtu.edu.cn

ity monitoring system is created based on fuzzy logic. This system is useful in evaluating nugget sizes and proposing possible causes for the variation in nugget sizes. In case of expulsion, the system can also detect the strength of expulsion, the time at which the expulsion occurs, and the possible causes for it.

Key words: aluminum alloy; resistance welding; electromagnetic force; evaluation index; quality monitoring of spot welding

Development of a new AgCuZnSn filler metal for brazing TNi shape memory alloy and stainless steel LI Ming-gao, SUN Da-qian, QIU Xiao-ming, LIU Wei-hong (School of Materials Science and Engineering, Jilin University, Changchun 130025, China). p44 - 48

Abstract: A new-type AgCuZnSn filler metal suitable for brazing TNi shape memory alloy and stainless steel and applying in biomedicine field has been developed. The melting characteristics, microstructure and brazing properties of AgCuZnSn filler metals were investigated and mechanical properties of the joints of TNi shape memory alloy and stainless steel brazed with AgCuZnSn filler metals were evaluated. The results showed that the liquidus and solidus temperatures of the novel Ag51 ~ 53Cu21 ~ 23Zn17 ~ 19Sn7 ~ 9 filler metal were 590.0℃ and 635.3℃, respectively. The filler metal mainly consisted of α-Ag solid solution, α-Cu solid solution and Ag-Cu eutectic phase as well as a little $Cu_{41}Sn_{11}$, AgZn, Ag_3Sn and Cu_5Zn_8 compounds. The tensile strength of the brazed joint of TNi shape memory alloy and stainless steel using the filler metal reached to 320 ~ 360MPa while the loss of shape memory effect and superelasticity of TNi shape memory alloy was low. The developed AgCuZnSn filler metal had advantage of low melting point, brazing metallurgy characteristics and interface metallurgy unity and the brazed joint had good tenacity and plasticity.

Key words: Ag-based filler metal; melting point; microstructure; TNi shape memory alloy; stainless steel

Finite element method analysis of temperature field in keyhole plasma arc welding WANG Hua-igang, WU Chuan-song, ZHANG Ming-xian (Shandong University, Jinan 250061, China). p49 - 53

Abstract: The models of both heat source and welding temperature field were developed according to the characteristic of keyhole plasma arc welding (K-PAW) process. The result of numerical simulation indicated that neither general double ellipsoidal heat source nor three dimensional conical heat source could precisely describe the thermal process in K-PAW. A modified model of three dimensional conical heat source was put forward. It could be used to calculate the weld width on both the top and the bottom surfaces of the workpiece exactly. But for the fusion line, the calculating precision was lower. Based on the theoretical analysis of keyhole and weld pool behaviors, a novel heat source model was employed which considered the combined action of both heat and force from the plasma arc. Finite element analysis of the temperature fields in K-PAW was conducted, and the calculated geometry result of K-PAW weld geometry was in agreement with experimental result.

Key words: plasma arc welding; keyhole; model of heat source; temperature field; finite element analysis

Effect of Nb and Cu metal layer thickness on microstructure and property of Si_3N_4/Nb/Cu/Ni/Inconel600 joint YANG Min, ZOU Zeng-da, QU Shi-yao, WANG Yu-fu (School of Materials Science and Engineering, Shandong University, Jinan 250061, China). p54 - 58

Abstract: Partial liquid phase diffusion bonding (PLPDB) of Si_3N_4 to Inconel600 high temperature alloy was carried out by using the interlayer of Nb/Cu/Ni foil. The main processing factors had been highlighted for the strength of Si_3N_4/Nb/Cu/Ni/Inconel600 system. Optimum parameters had been obtained as bonding temperature 1 403 K, bonding time 50 min and bonding pressure 7.5 MPa. Effects of Cu and Nb metal layer on the microstructure and properties of joint were respectively investigated by changed thickness of Nb and Cu layer. Test results showed that while the thickness of Cu layer was thinner than 0.05 mm, the strength of joint increased fast with the increase of Cu layer thickness, but when the thickness surpassed 0.05 mm, the strength of joint increased slowly with the increase of Cu layer. When the thickness of Nb layer increased, the thickness of reaction layer increased, but the strength of Si_3N_4/Nb/Cu/Ni/Inconel600 joint increased firstly to a maximum value, then decreased.

Key words: partial liquid phase diffusion bonding (PLPDB); Si_3N_4 ceramics; Inconel600 high temperature alloy; interlayer

Scanning electron beam processing technology based on programmable control LI Shao-qing, WANG Xue-dong, ZHANG Yu-xia, YAO Shun (Welding Engineering Institute, Shanghai Jiaotong University, Shanghai 200030, China). p59 - 62, 66

Abstract: A general vacuum electron beam (EB) machine was equipped with a control system of electron beam scanning which consisted of two electron beam deflection coils, industrial personal computer (IPC), multifunctional DAQ (data acquisition) card, power amplifiers, programmable logic controller (PLC), virtual instruments (VI) software LabVIEW and so on. The EB scanning track, scanning frequency and energy density distribution at heating zone could be programmed off-line and adjusted on-line. Brazing experiment of stainless steel capillary tube-to-plate structure was carried out by means of the system, and the quality of brazed joints met the technical specification of structure. Dissimilar alloys like niobium and titanium were welded using the scanning heating mode of dissymmetric heat input. The joint was found that melted niobium amount was as much as titanium, and the weld shape was almost symmetric. Dissimilar metals that couldn't be welded directly such as Re-Ti might be

welded by using scanning heating technology to prepare the powder metallurgical transition layer.

Keywords: electron beam (EB); scanning control system; scanning track; energy control

Diffusion bonding of TC4/Ni/QAl10-3-1.5 GUO Wei[1], ZHAO Xi-hua[1], SONG Min-xia[1], FENG Ji-cai[2], YANG Biao[1] (1. School of Material, Jilin University, Changchun 130025, China; 2. State Key Laboratory of Advanced Welding Production Technology, Harbin Institute of Technology, Harbin 150001, China). p63 – 66

Abstract: TC4 and QAl10-3-1.5 were diffusion-bonded with Ni interlayer. The diffusion-bonded joints were evaluated by scanning electron microscopy (JEOL JSM-6700F) and its attaching energy dispersive spectroscopy (EDS). Intermetallic compounds at the interface were detected vie X-ray diffraction (XRD) and microhardness tests and tensile testings were done to evaluate the properties of bond joints. The results indicated that TC4 and QAl10-3-1.5 with Ni interlayer were bonded firmly under the condition of 870℃ temperature, 10MPa bond stress and 60min holding time, and the bond strength was up to 325MPa; furthermore, various reaction bands appeared in the diffusion zone, and NiTi phase, (NiTi + Ni_3Ti) phase and Ni(Cu) solid solution were produced at the interface zone.

Keywords: diffusion bonding; titanium alloy; copper alloy; Ni interlayer; microstructure

Soldering of LD31 aluminum alloy with electro brush plated Sn-Pb alloys ZHAO Zhen-qing[1], WANG Chun-qing[1], DU Miao[2], HUANG Yi[1] (1. Harbin Institute of Technology, Harbin 150001, China; 2. Harbin Welding Institute, Harbin 150080, China). p67 – 70, 74

Abstract: The bonding of LD31 aluminum alloy with electron brush plated Sn-Pb solder after the deposition of Ni and Cu transient layers was investigated in this paper. The influence of electric deposition parameters of SnPb alloy on the coating quality and subsequent solderability was studied. The constitution of coatings, the morphology of Sn-Pb coating, the bonding mechanism in the soldering and the elements distribution in the soldered joint were studied by scanning electron microscope, energy dispersive X-ray analysis and metallographic analysis. The results of soldering experiment showed that after the deposition of Ni and Cu coatings, the bonding of LD31 aluminum alloy could be transformed to the bonding of copper, and the bonding of coatings could bear the heating condition in the soldered. The shear strength of the soldered joint could reach as high as 20MPa.

Keywords: LD31 aluminum alloy; electron brush plating; coating; soldering

Particularity analysis of Francis turbine runner's simulation during welding JI Shu-de, FANG Hong-yuan, LIU Xue-song, MENG Qing-guo (Harbin Institute of Technology, Harbin 150001, China). p71 – 74

Abstract: Aiming at the particularity of Francis turbine runner's simulation in the process of welding, the method was adopted which solved the loading of welding thermal source by means of node-to-node connection and the method was brought forward which solved the problem of weld's wire feed by dividing the weld into many parts. These two methods were proved reasonably by the runner's temperature field. Moreover, the problem of heat conduction between independent entities and the problem of heat elimination between blade and air were successfully solved by using contact bodies. It had important guiding significance to the numerical simulation of complicated weldments.

Keywords: runner; welding; numerical simulation; temperature field

Optimization of water dissolution modification process using silver brazing fluxes CHEN Hai-yan, LI Wei-min, LI Feng, SHU Chang (Faculty of Material and Energy, Guangdong University of Technology, Guangzhou 510643, China). p75 – 76, 80

Abstract: The optimization of the water dissolution process using silver brazing fluxes was conducted by orthogonal test. The test result showed that effect of bake time on flux property is the best notable, next proportioning of compositions affected flux property, then bake temperature affected flux property. The optimum process parameters are component of 42% KF + 23% KBF_4 + 35% B_2O_3, bake time of 45min and bake temperature of 350℃. By using the silver brazing fluxes, the best results of the jointing can be carried out.

Key words: silver brazing flux; orthogonal test; absorptivity; melting point; spreading property

Modeling of welding pool surface reflectance of aluminum alloy pulse GTAW LI Lai-ping, CHEN Shan-ben, LIN Tao (School of Materials Science and Engineering, Shanghai Jiaotong University, Shanghai 200030, China). p77 – 80

Abstract: The key to the surface height calculation of pulse GTAW welding pool based on shape from shading (SFS) is to build up a surface model of welding pool. Based on the imaging characteristics of aluminum alloy pulse GTAW welding pool, the surface reflectance model is built after analyzing arc intensity, filter system, welding pool shape and reflectance characteristics. With smooth constraint condition of the welding pool surface and variable factor successive over relaxation (SOR) method, the height of welding pool surface is calculated and the error is analyzed.

Key words: aluminum alloy pulse GTAW; surface reflectance model of welding pool; shape from